J Mater Sci (2008) 43:4870–4875
DOI 10.1007/s10853-008-2708-9

Effect of yttrium additions on the properties of grain-refined Mg–3%Nd alloy

Eli Aghion · Yael Gueta · Nir Moscovitch · Boris Bronfin

Received: 17 February 2008 / Accepted: 6 May 2008 / Published online: 3 June 2008

Abstract A systematic study was carried out to evaluate the effect of up to 2.5% yttrium additions on the properties of Mg–3%Nd alloy designated for high-temperature gravity casting applications. All the tested alloys were grain-refined by zirconium. The results show that additions of yttrium significantly improved the tensile yield strength, fatigue strength, and creep resistance while reducing the ductility. However, other properties such as the ultimate tensile strength and corrosion resistance in 5% NaCl solution were nearly not affected. The strengthening effect obtained by the yttrium additions is explained in terms of solid-solution strengthening and due to formation of a ternary phase of Mg–Nd–Y. The improved creep resistance was due to the large solubility of yttrium in solid-solution magnesium matrix and to the effective creep deformation barriers created by the ternary phase. The casting performance of the tested alloys in terms of fluidity was similar and no significant effect of the yttrium was evident

Introduction

The attractiveness of magnesium alloys as structural materials in applications requiring weight savings is due to increasing environmental concern. This is mainly seen in the automotive and aerospace industries that need to reduce fuel consumption because of increasing cost and to address greenhouse gas emissions requirements [1–4]. Currently, although the leading production technology of magnesium components is die casting, there is a growing interest in the use of affordable magnesium alloys for gravity and permanent mold casting. In particular, the interest is focused on magnesium alloys that offer high creep resistance for engine and powertrain applications. One of the traditional alloys commonly used for these applications is WE43 that contains 4% yttrium and 3% rare earth-mischmetal elements such as Gd, Dy, and Yb. However, the relative high cost of this alloy and its limited castability have restricted its practical use for applications relating to racing automotive industries and helicopters [5].

This report describes a study of the Mg–3%Nd with small additions of Y and refined with zirconium. This system was selected because of the relative availability of Nd, its effectiveness on magnesium properties, and the potential beneficial effect of Y. Neodymium is a common rare earth alloying element choice for magnesium due to the optimum combination of its wide solubility range in solid magnesium and its relatively low cost [6]. Yttrium, on the other hand, has a more significant beneficial effect on properties compared with other rare earth alloying elements but can reduce melt castability at concentrations higher than 3%. The fact that Y has a considerably higher solubility in magnesium compared with Nd may indicate that its use in combination with relatively small quantities of Nd have a synergistic beneficial effect on magnesium's properties. The use of zirconium as an additional additive to the ternary Mg–Nd–Y alloying system is due to its unique refining capabilities. Zirconium also has a beneficial effect on the corrosion resistance and level of porosity in magnesium casting. The more effective refining effect of Zr is obtained when the magnesium melt has been saturated with this element at a temperature exceeding 750 °C.

E. Aghion (✉) · Y. Gueta
Department of Materials Engineering, Ben Gurion University, P.O. Box 653, Beer Sheva 84105, Israel
e-mail: egyon@bgu.ac.il

N. Moscovitch · B. Bronfin
Dead Sea Magnesium Ltd, Beer Sheva, Israel

Although studies have been published about the phase composition and precipitation reactions in Mg–RE–Y alloys, the particular effect of Y on the obtained properties is not yet fully understood [7–9]. The aim of the present study was to evaluate and explain the effect of up to 2.5% Y additions on the properties of Zr-refined Mg–3%Nd alloy. Pure Nd and a reduced quantity of Y as alloying elements were used to characterize affordable material systems for practical applications.

Experimental procedure

The preparation of the tested alloys was carried out according to the following procedure. Pure magnesium grade 9980A ingot was melted in a low-carbon steel crucible with a protective gas atmosphere of $CO_2 + 0.5\%$ SF_6. The melt was then superheated to 775 °C before pure Nd and commercially pure Zr were added. These were added while the molten metal was under intensive stirring, for up to 25 min to insure complete dissolution of the alloying elements. After the element addition and stirring, the melt was held quiescent for up to 40 min to allow proper settling of heavy substances such as iron and magnesium oxides. Following settling, various quantities of Y were added according to the required compositions. The addition of Y was carried out by gentle agitation to insure the dissolution of Y and to reduce the reaction between Y and iron that is generated from the crucible walls which can result in unnecessary loss of Y. After the addition of the Y, the melt was held quiescent for up to 1 h for final settling of iron and non-metallic inclusions and to insure proper homogenization of the molten material. Following this stage, the molten alloy was gravity cast into a cylindrical steel die to obtain bars15 mm in diameter with 150 mm length. The chemical compositions of the obtained alloys, which were determined using a Baird Spectrovac 2000 spark spectrometer, are shown in Table 1.

ASTM specimens for tensile, creep, and fatigue testing were machined from the cast bars. To insure adequate soundness of the specimens before testing, all the specimens were evaluated by X-ray radiography using a Seifert Eresco 200MF constant potential X-ray tube. The specimens were also T6 heat treated using the following procedure: solution treatment at 540 °C for 5 h, quenching in hot water at 80 °C, and aging at 250 °C for 3.5 h. This heat treatment procedure was adopted to implement all the advantages obtained by the precipitation hardening mechanism.

The T6 age hardening heat treatment also ensures an optimum combination of mechanical strength and high temperature performance in terms of creep resistance [9].

Microstructure analysis of the alloys was performed using optical microscopy, scanning electron microscopy (JEOL-JSM-5410), and high-resolution scanning electron microscopy (JEOL 7400F). Phase identification was obtained by X-ray diffraction analysis using a DMAX-2100 with Cu Kα wavelength.

The tensile tests were carried out at room temperature using an Instron 4483.

Fatigue strengths were obtained using rotating beam cyclic loading at $R = -1$ for 10^8 cycles. Creep tests were carried out at 200 °C at 100 MPa load using a SATEC M-3 creep machine. The corrosion rate measurements were obtained by immersion tests in 5% NaCl solution for 72 h according to ASTM standard G31-87. The corrosion samples having 10 mm diameter and 100 mm length were machined from the T6-treated bars.

The casting performance of all the tested alloys, in terms of comparative fluidity, was obtained using the spiral mold testing apparatus shown in Fig. 1. According to this method, the fluidity was evaluated by the length of the casting spiral obtained under the same permanent mold-casting conditions. Increased spiral length was indicative of improved fluidity.

Table 1 Chemical composition of tested alloys (wt.%)

Alloy No.	Nd	Zr	Y	Si	Fe	Cu	Ni
1	3.1	0.46	–	0.01	0.004	0.001	0.001
2	3.1	0.49	0.48	0.01	0.003	0.001	0.001
3	2.9	0.44	0.95	0.01	0.004	0.001	0.001
4	3.0	0.43	1.45	0.01	0.003	0.001	0.001
5	3.1	0.46	1.95	0.01	0.003	0.001	0.001
6	3.0	0.48	2.45	0.01	0.004	0.001	0.001

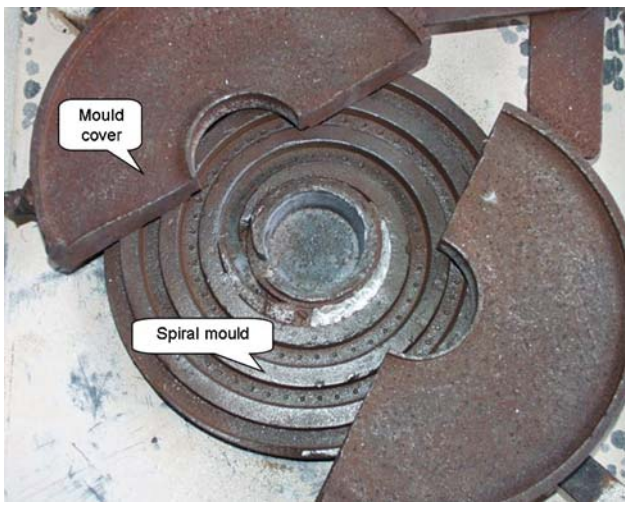

Fig. 1 Spiral mold-casting apparatus for comparative fluidity analysis

Results and discussion

Typical microstructures and X-ray diffraction analysis results for alloys 1 and 5 in as-cast conditions and after T6 heat treatment are shown in Figs. 2, 3 and 4, respectively. These reveal that both alloys have similar microstructure appearance as both systems comprise a solid-solution magnesium matrix and a secondary-phase precipitate. The HRSEM analysis of alloy 5 after T6 heat treatment, Fig. 3, clearly revealed the presence of elongated ternary β'-phase within the Mg grains. The X-ray diffraction analysis of the two alloys in the as-cast condition, Fig. 4, indicates that the microstructure is mainly composed of a magnesium matrix and Mg_3Nd precipitate. The dominant presence of Mg_3Nd precipitate is in line with the thermodynamic analysis of Meng et al. [10] showing that Mg_3Nd has the greatest relative stability in the Mg–Nd system compared with other possible compounds such as $Mg_{12}Nd$, $Mg_{41}Nd_5$, Mg_2Nd, and MgNd. On the other hand, the diffraction pattern of alloy 5, Fig. 4b, shows the presence of a modified secondary precipitate phase, which we have entitled β-phase following the work of Meng et al. [11]. Meng identified this phase in the ternary system Mg–Nd–Y; the obtained β-phase being a ternary phase with the basic semi-stoichiometric formula of $Mg_p(Nd,Y)_q$ where $p + q$ is set to 1. This is based on the fact that the binary phase Mg_3Nd obtained in the Mg–3%Nd system has an extensive solubility for a third element. Hence, when Y is added, the Mg_3Nd phase is modified to the ternary phase $Mg_p(Nd,Y)_q$. Distinguishing between the binary phase Mg–3%Nd and the ternary phase $Mg_p(Nd,Y)_q$ by metallography is quite difficult, as the morphology of both phases are very similar.

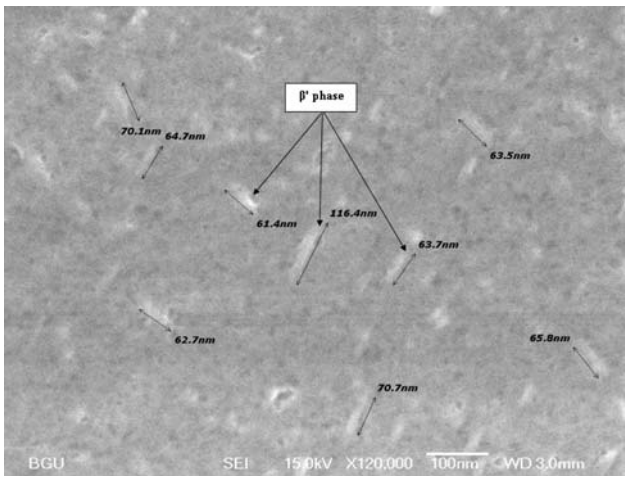

Fig. 3 HRSEM microstructure of alloy 5 after T6 heat treatment

In addition, it should be pointed out that due to the extensive solubility of Y in magnesium it is assumed that a significant portion of the Y is dissolved in the magnesium-based solid-solution. Hence, it is believed that the Y added to Mg–3%Nd is being partitioned between the two phases. The major part of the Y is dissolved in the magnesium matrix while a relatively small quantity of Y is dissolved in the binary phase Mg_3Nd. The addition of Y to that phase results in the formation of the ternary β-phase.

The effects of Y additions on the ultimate tensile strength, tensile yield strength, elongation, and fatigue strength of Mg–3%Nd after T6 heat treatment are shown in Figs. 5, 6, 7, and 8, respectively. It is evident from the results that Y has a significant beneficial effect on the tensile yield strength and fatigue strength, Figs. 6 and 8.

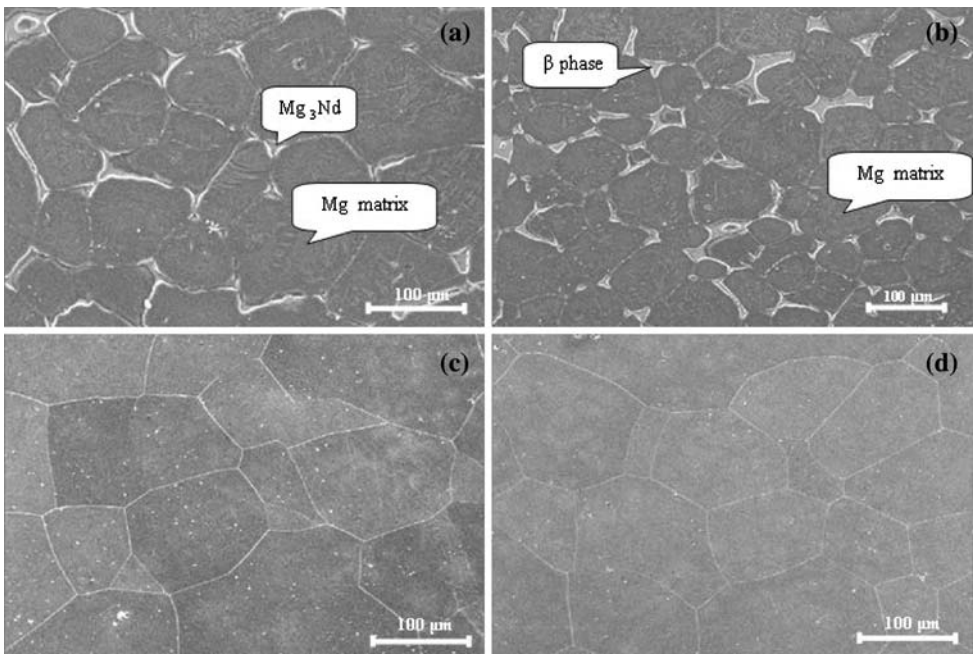

Fig. 2 Typical microstructure obtained by optical and SEM microscopy of (**a**) and (**b**) alloys 1 and 5, respectively, in as-cast conditions, (**c**) and (**d**) alloys 1 and 5, respectively, after T6 heat treatment

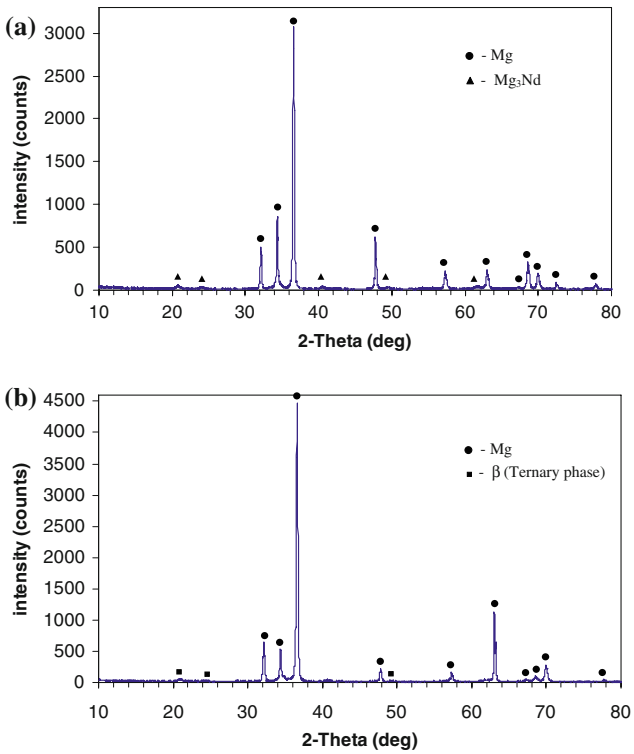

Fig. 4 X-ray diffraction analysis in as-cast condition of (**a**) alloy 1 and (**b**) alloy 5

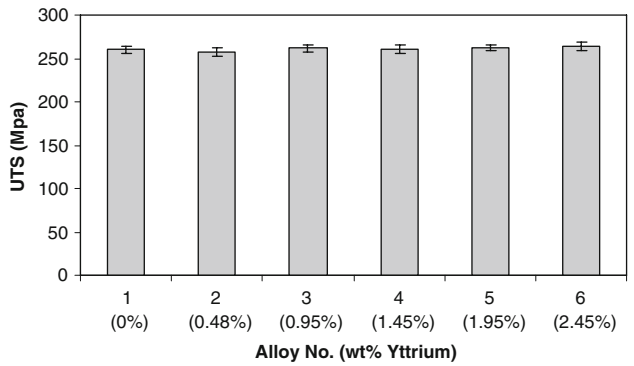

Fig. 5 Ultimate tensile strength (UTS) at room temperature of alloys 1–6 (with indicated yttrium content)

However, it has a minor effect on the ultimate tensile strength, Fig. 5, and a detrimental effect on elongation, Fig. 7.

Based on the obtained microstructure analysis and previous publications [12–14], these results can be explained by a simple strengthening mechanism that is schematically illustrated in Fig. 9. According to this mechanism, the strengthening effect of Y after T6 heat treatment is implemented by two different means: solid-solution strengthening due to the significant high solubility of Y in magnesium and precipitation strengthening due to the formation of a fine

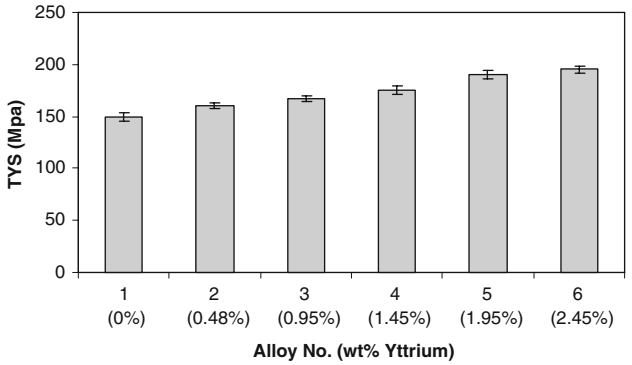

Fig. 6 Tensile yield strength (TYS) at room temperature of alloys 1–6 (with indicated yttrium content)

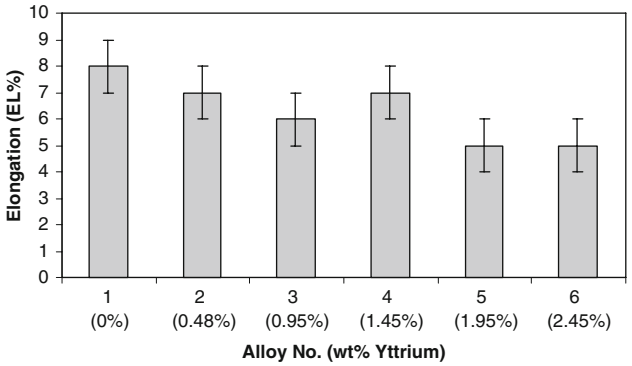

Fig. 7 Elongation (EL%) at room temperature of alloys 1–6 (with indicated yttrium content)

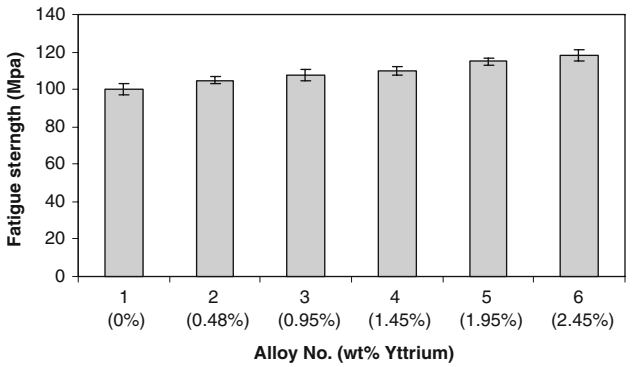

Fig. 8 Fatigue strength at room temperature of alloys 1–6 (with indicated yttrium content)

dispersed ternary β'-phase intermetallic phase. Hence there is a possibility that the high solubility of Y in the magnesium matrix and in the ternary β'-phase can create a continuous pattern of Y that improves the physical bonding between the matrix and the ternary phase. This Y base pattern may enhance the coherency between the ternary β'-phase and the magnesium solid-solution matrix as a result of improved atom matching at the interface between those two phases. Consequently, the coherent interface acts as an effective

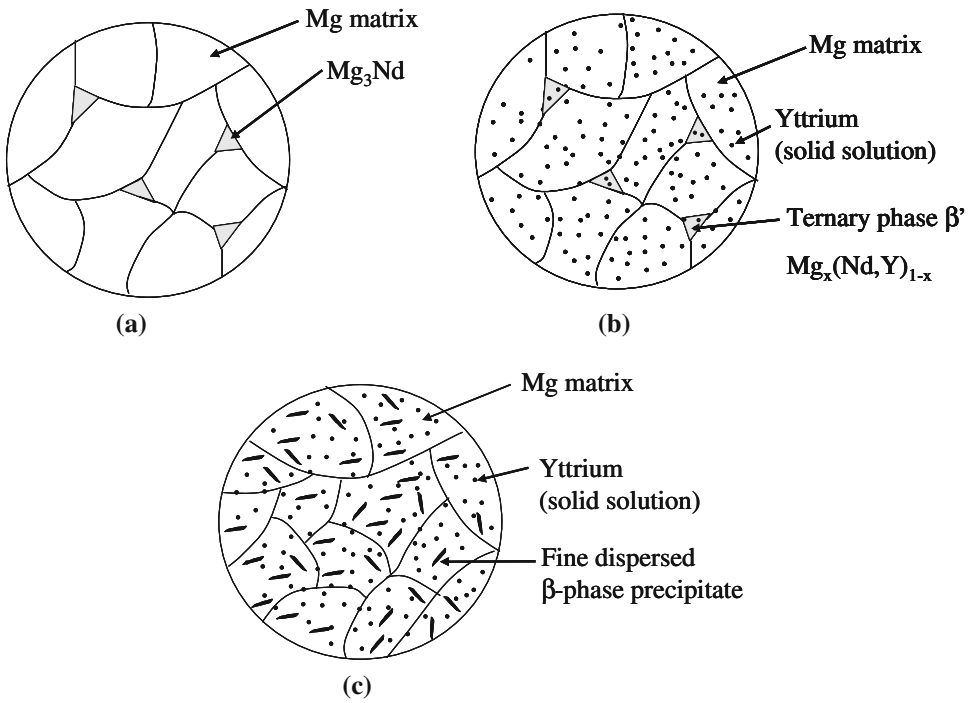

Fig. 9 Schematic illustration of the strengthening mechanism of yttrium in Mg–3%Nd. (**a**) Mg–3%Nd in as-cast condition, (**b**) Mg–3%Nd–2%Y in as-cast condition, and (**c**) Mg–3%Nd–2%Y after T6 heat treatment (all numbers relates to wt.%)

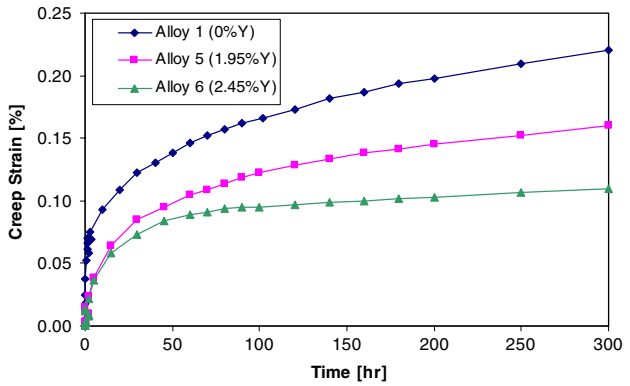

Fig. 10 Creep resistance of alloys 1, 5, and 6 (with indicated yttrium content in wt.%). Test temperature: 200 °C, constant load: 100 MPa

barrier to dislocations flow and hence results in improved tensile and fatigue strength while ductility is being reduced.

The effect of Y additions on the creep resistance of Mg–3%Nd is shown in Fig. 10. Additions of Y have significantly improved the creep resistance. It is assumed that the formation of the ternary β-phase in the form of a fine dispersion intermetallic phase creates improved barriers to dislocation creep mechanism. In addition, the dissolved Y in the magnesium solid-solution matrix has a beneficial effect on the creep resistance mainly due to locking effect of Y with respect to dislocation creep mechanism.

The corrosion performance of Mg–3%Nd alloys with various Y contents in 5% NaCl solution is shown in Table 2; there is a minor effect of Y on the corrosion rate. Based on the findings of Ghali et al. [15] and Zucchi et al. [16] it is believed that the dominant beneficial effect on the corrosion performance of Mg–3%Nd with up to 2.5% Y is controlled by the presence of Nd. Hence the effect of yttrium in the ternary system Mg–Nd–Y is comparatively insignificant.

Table 2 Corrosion rate of alloys 1–6 (with indicated yttrium content), after 72 h immersion test in 5% NaCl solution

Alloy No.	1	2	3	4	5	6
(wt.% yttrium)	(0)	(0.48)	(0.95)	(1.45)	(1.95)	(2.45)
Corrosion rate (mpy)	35 ± 4	37 ± 5	32 ± 5	38 ± 3	34 ± 6	33 ± 4

Table 3 Casting performance of Mg–3%Nd with various quantities of yttrium, obtained in terms of spiral length

Alloy No.	1	2	3	4	5	6
(wt% yttrium)	(0)	(0.48)	(0.95)	(1.45)	(1.95)	(2.45)
Spiral length (mm)	215	215	220	225	225	220

The casting performance of Mg–3%Nd alloy with up to 2.45% Y in terms of fluidity, as measured by spiral length, is shown in Table 3. The minor effect of Y on the fluidity is probably related to the larger solubility of this element in magnesium.

Conclusions

The present investigation clearly demonstrates the beneficial effect of yttrium additions on the tensile yield strength,

fatigue strength, and creep resistance of Mg–3%Nd alloy. These beneficial effects were obtained without deteriorating the fluidity of the tested alloys during gravity-casting process.

The strengthening effect caused by yttrium resulted in a relatively small reduction in ductility. The corrosion performance of Mg–3%Nd alloys in 5% NaCl solution was nearly unaffected by the addition of yttrium.

References

1. Blawert C, Hort N, Kainer KU (2004) Trans Indian Inst Met 57:397
2. Cole GS (2007) In: Beals RS, Luo AA, Neelameggham NR, Pekguleryuz MO (eds) Magnesium technology 2007. TMS, Orlando, FL
3. Beals RS, Liu Z-K, Jones JW et al (2007) JOM 59:43. doi:10.1007/s11837-007-0103-7
4. Beals RS, Tissington C, Zhang X et al (2007) JOM 59:39. doi:10.1007/s11837-007-0102-8
5. Lambri OA, Riehemann W, Salvatierra LM et al (2004) Mater Sci Eng A 373:146. doi:10.1016/j.msea.2004.01.020
6. Bronfin B, Moscovitch N (2006) Met Sci Heat Treat 48:479. doi:10.1007/s11041-006-0121-z
7. Apps PJ, Karmizadeh H, King JF et al (2003) Scripta Mater 48:475. doi:10.1016/S1359-6462(02)00509-2
8. Mordike BL (2001) J Mater Proces Technol 117:391. doi:10.1016/S0924-0136(01)00793-2
9. Apps PJ, Karmizadeh H, King JF et al (2003) Scripta Mater 48:1023. doi:10.1016/S1359-6462(02)00596-1
10. Meng FG, Liu HS, Liu LB et al (2007) Trans Nonferrous Met Soc China 17:77. doi:10.1016/S1003-6326(07)60051-X
11. Meng FG, Wang J, Liu HS et al (2007) Mater Sci Eng A 454–455:266. doi:10.1016/j.msea.2006.11.048
12. Nie JF, Muddle BC (2000) Acta Mater 48:1691. doi:10.1016/S1359-6454(00)00013-6
13. Polmear IJ (1992) In: Mordike BH, Hehman F (eds) Magnesium alloys and their applications. Garmish-Partenkirchen
14. Nie JF (2002) In: Kaplan HI (ed) Magnesium technology 2002. TMS, Seattle, WA
15. Ghali E, Dietzel W, Kainer KU (2004) J Mater Eng Perform 13:7. doi:10.1361/10599490417533
16. Zucchi F, Grassi V, Frignani A et al (2006) J Appl Electrochem 36:195. doi:10.1007/s10800-005-9053-3